



A Pilot Study of Mercury Distribution in the Carapace of Four Species of Sea Turtles from Northeastern Brazil

César Augusto Barrios-Rodríguez¹ · Luiz Drude de Lacerda¹ · Moises Fernandes-Bezerra¹

Received: 20 December 2022 / Accepted: 19 May 2023 / Published online: 27 May 2023
© The Author(s), under exclusive licence to Springer Science+Business Media, LLC, part of Springer Nature 2023

Abstract

Scutes present very complex morphologies with different growth rates at different areas of the carapace that can change the accumulation process of essential and non-essential metals. To infer the effects of morphology and growth on Hg concentrations in scutes, we mapped them in the carapace of one individual of four species of sea turtles sampled along the Brazilian coast. The results showed that Hg concentrations were higher in the vertebral scutes of *Chelonia mydas* and *Eretmochelys imbricata* suggesting variation in growth rates of different carapace areas since the vertebral area is the first to develop prior to costal areas. *Caretta caretta* and *Lepidochelys olivacea* did not show differences between carapace areas. The preliminary data from this pilot study indicate that vertebral scutes may be suitable for monitoring Hg in *C. mydas* and *E. imbricata*, since they reflect longer exposure period. A species-to-species comparison of Hg concentrations is not possible due to the small number of sampled individuals, nevertheless, *E. imbricata* showed remarkably lower Hg concentrations compared to the other three species. Further studies are required for all four species, with a larger number of individuals, preferentially of varying life stages, due to the unknown effects of different diets, Hg exposure, and migration histories.

Keywords Mercury · Sea turtles · Biomonitoring · Carapace · Scutes

Introduction

The ubiquitous presence of mercury (Hg) in the oceans triggered many studies aimed to understand the impact generated by anthropogenic Hg on the marine biota. In this sense, the use of biological biomonitors has been a valuable tool to monitor and assess spatial and temporal trends of Hg concentrations but also because organisms respond to the biological available Hg fraction allowing a direct association with exposure risk and toxicity (Needham et al. 2008; Evers et al. 2018).

Widely distributed, long-live species, such as sea turtles, have a lifespan compatible with the residence time of Hg in the oceans, being especially interesting for biomonitoring purposes (Evers et al. 2018). However, targeting these

animals requires the use of non-invasive sampling methods that allow the quantification of Hg without euthanizing the individuals of these endangered species (Bezerra et al. 2012; Rodriguez et al. 2019). Many authors worldwide (Sakai et al. 2000; Day et al. 2005; Bezerra et al. 2012, 2013) have successfully used scutes to monitor Hg in these chelonians. For example, scutes were used to characterize bioaccumulation and patterns of temporal exposure to Hg and other trace metals in sea turtles (Schneider et al. 2015; Bezerra et al. 2015; Barraza et al. 2019; Villa et al. 2019) collected for two populations of *C. mydas* from a foraging ground within the Great Barrier Reef (Howick Island group) as well as from Shoalwater Bay in Australia and their results provided robust proxies of exposure conditions. Similarly, Hg concentrations in scutes reflected exposure levels in *C. caretta* from different nesting areas in northeastern Brazil (Barrios et al. 2019).

Sea turtle carapace scutes grow in a layered pattern and with multiple growth areas (Achrai and Wagner 2013), because of that, the accumulation of elements can vary across carapace areas (Day et al. 2005; Mattei et al. 2015). Structurally, the carapace is subdivided into four areas and

✉ César Augusto Barrios-Rodríguez
hpbarrios15@gmail.com

¹ Laboratório de Biogeoquímica Costeira, Instituto de Ciências do Mar, Universidade Federal do Ceará, Av. Abolição, 3207, Fortaleza, Ceará 60165-081, Brasil

each with a specific number of scutes depending on the species (Wyneken 2001). It also presents many submicron layers stacked to form sulfur-rich keratinous scutes that cover the dorsal bone. Some of the most essential components of scutes are amino acids such as cysteine, which provide stiffness and strength to the scute structure (Achrai and Wagner 2013). Cysteine, the only proteinogenic thiol-containing amino acid, and its side chain is the principal coordination site for Hg^{+2} , as well as organic species like methylmercury. In addition, Hg ions can even be occluded within disulfide bridges connecting adjoining polypeptide chains. This high affinity of Hg to the thiol group helps the formation of chelating agents immobilizing Hg and eventually serving as a detoxification mechanism (Warner and Jalilvand 2016 and references therein), as well as potentially providing a record of the feeding-related Hg incorporation (Toni et al. 2007; Schneider et al. 2015). The strong binding capacity of Hg^{+2} is in agreement with the relatively low (< 5%) proportion of methyl-Hg previously reported in scutes of some of the studied species (Barrios et al. 2019).

Since its formation, the carapace shows quite complex aspects that may influence the accumulation of Hg as well as other essential and non-essential metals. The carapace of sea turtles, except for the leatherback (*Derموchelys coriacea*), not included in this study, is composed of vertebral scutes (V), right costal scutes (RCS), left costal scutes (LCS), left marginal scutes (LMS), and right marginal scutes (RMS). The number of scutes in each of these positions varies according to the species. Therefore, to understand how much variation exists within a single individual, this paper maps the Hg concentrations across the vertebral, costal, and marginal areas of the carapace in four species of sea turtles, occurring along the Brazilian northeastern coast.

Materials and Methods

All procedures and analyzes were carried out within the current norms of the Brazilian environmental legislation, under the authorization of the System of Authorization and Information in Biodiversity - SISBIO, License No. 66,837 and 66,088 (2022) from the Ministry of the Environment.

Sampled individuals were found dead on the beach between 2019 and 2020. Scutes samples were collected from the carapace of four sea turtles in the coastal region of Ceará (Praia do Futuro, 3°44'56" S, 38°26'48" W) (green turtle, *Chelonia mydas* and loggerhead turtle, *Caretta caretta*) and of Pernambuco (Porto de Galinhas, 8°29'45" S, 34°59'37" W) (hawksbill turtle, *Eretmochelys imbricata* and olive ridley sea turtle, *Lepidochelys olivacea*). All locations are in northeastern Brazil (Figure S1). The areas of Pernambuco and Ceará are important nesting and feeding

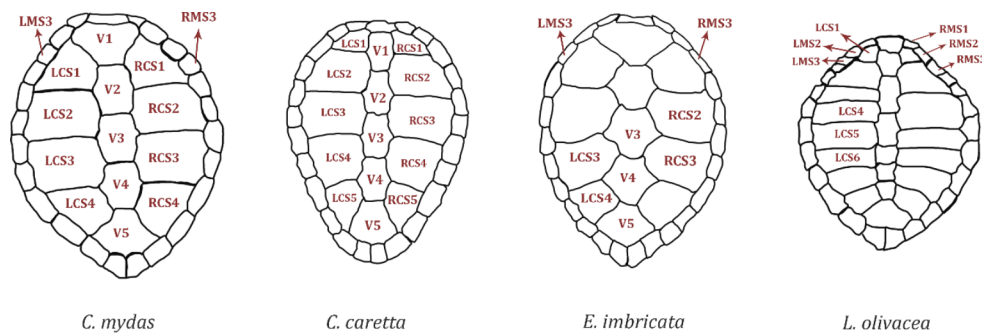
sites for *C. caretta* and *E. imbricata* (Marcovaldi et al. 2010; Moura et al. 2012). In the case of *C. mydas*, although its priority spawning areas are located on oceanic islands (Bellini et al. 2013), the non-reproductive individuals, especially juveniles, use foraging grounds along the Brazilian coast (Proietti et al. 2009). The presence of dead individuals of *L. olivacea*, on beaches of Pernambuco, a species which occurs mostly on offshore areas, has been associated with incidental capture by the pelagic longline fishery (Sales et al. 2008). Environmental Hg levels reviewed by Marins et al. (2004) shows Pernambuco with higher degree of contamination, based on geoaccumulation index, due to industrial effluents, compared to Ceará coast, that shows lowest contamination index.

The individuals were classified as adult, subadult, and juvenile based on carapace size, suggesting a similar omnivorous diet (Bjorndal 1997; Vélez-Rubio et al. 2016). *C. mydas* is the only species to present an ontogenetic diet change during its growth, being omnivorous in the juvenile phase and herbivorous in the adult phase. Thus, according to studies that report an omnivorous diet in individuals smaller than 50 cm (Velez-Rubio et al. 2016), the individual used in this study probably also had an omnivorous behavior. Sex could not be determined. However, available studies on the Hg distribution between males and females in the four species showed no significant differences in Hg concentrations (Bruno et al. 2021, and references therein). Therefore, we do not consider these variables to affect the observed Hg concentrations.

Curved carapace length (CCL) and curved carapace width (CCW) were recorded for each individual. Stranded animals were in different decomposition states, especially those from Pernambuco to a point to avoid sampling most scutes showing visual signs of structural alteration. Fortunately, those from Ceará were of recently dead animals with the entire carapace intact. The rarity of stranded animals, abrasion, and scavengers hampered the sampling of a larger number of animals.

The scutes were collected by carefully scrapping only the keratinized layer, with a dissection knife, avoiding the skin and dermis tissues. Since the number of scutes in each of position of the carapace varies according to the species our sampling strategy reflected these differences (Fig. 1). Two samples were collected from each scute. In *C. mydas*, five vertebral scutes, four right costal scutes, four left costal scutes, one right and one left marginal scutes were collected (n=30). In *C. caretta*, five vertebral scutes, five right and five left costal scutes were collected (n=30). In *E. imbricata*, three vertebral scutes, two right and two left costal scutes, one right and one left marginal scutes were collected (n=14). In *L. olivacea*, four left costal scutes, three right, two left marginal scutes were collected (n=18). In the case

Fig. 1 Sampling map of carapace scutes in the four species of sea turtles. V: Vertebral, RCS: Right Costal Scutes, LCS: Left Costal Scutes, RMS: Right Marginal Scutes, LMS: Left Marginal Scutes. For every scute sampled, two samples were collected from different areas of the scute



of *L. olivacea*, *E. imbricata*, and *C. caretta*, it was not possible to collect all scutes from each area because of limited time and available personnel. Although *E. imbricata* and *L. olivacea* were fresh dead individuals, some vertebral and lateral scutes were missing. In the case of *C. mydas*, it was not possible to sample all the scutes from the marginal region due to the small size of the individual.

After removal, scutes were carefully washed with distilled water, dried with clean tissue paper, and transported in iceboxes to the laboratory. Prior to analysis, scutes were rinsed with distilled water and scraped with a plastic scrubbing pad to remove any remaining particles, following the procedures detailed in Day et al. (2005). Scute samples were then soaked in 50 ml Milli-Q® water in a pre-cleaned glass vial and immersed in an ultrasound bath for 20 min. Finally, the samples were dried in an oven at 60 °C for 12 h for moisture removal.

For total Hg quantifications, samples (0.5 g d.w.) were placed in Teflon tubes containing 10 mL of concentrated nitric acid (HNO₃, 65%) for one-hour pre-digestion. Total sample digestion was carried out in a microwave furnace for 30 min at 200 °C. After cooling, 1 mL of hydrogen peroxide (H₂O₂, 35%) was added. The final extract was transferred and diluted in volumetric flasks to 100 mL, with Milli-Q® water. All materials that came into contact with the samples were washed with acid and duplicate procedural blanks were included in each digestion bath. The total Hg fraction obtained with this method includes all inorganic and organic Hg species present in scutes. Quantification of total Hg was obtained by cold vapor generation atomic absorption spectrophotometry (CV-ASS) in a NIC RA-3 (NIPPON®) spectrophotometer. The average linearity coefficient of the calibration curves (R²) obtained was 0.9998 ± 0.0001. The mean limit of detection (LOD) of the method was 0.03 ± 0.01 ng g⁻¹, calculated as three times the standard deviation of the reagent blanks divided by the slope of the calibration curve. The validation of the methodology was obtained by using certified reference material (fish muscle ERM-BB422), with a mean recovery of 92.1 ± 5.6% (n = 10).

Statistical analyses were performed using R 4.1.2 (R Development Core Team 2021). Data normality was tested

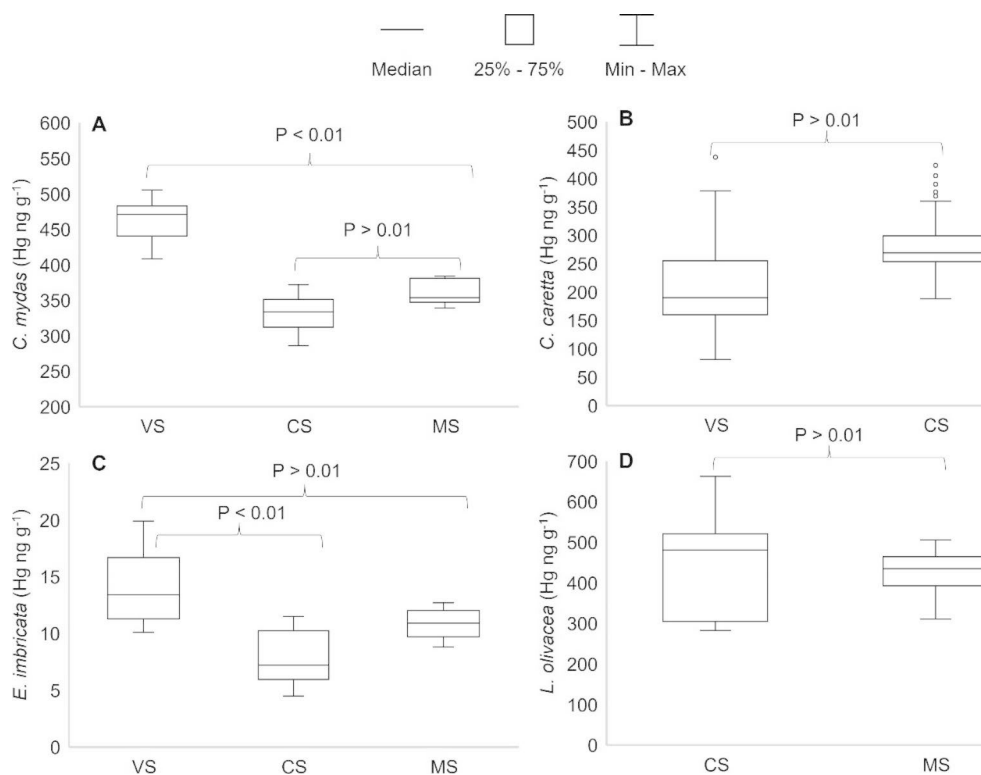
using the Shapiro-Wilk test. To test for differences in Hg concentrations between carapace areas (e.g., Vertebral, Costal, Marginal), parametric ANOVA tests and non-parametric Kruskal-Wallis tests were conducted according to conformity to normality assumptions. When differences were found to be significant, post hoc tests (Tukey's and Mann-Whitney's tests) were conducted to identify where Hg concentrations differ among carapace areas. All tests were conducted assuming a significance level of 99% (p < 0.01). All Hg levels are reported as ng g⁻¹ on a dry weight basis. For the statistical analyses were used the Hg concentrations for the two samples were collected from each scute.

Results

Biometric data of the sampled individuals vary according to species: *C. mydas* presented CCL of 38 cm and CCW of 35 cm, classified as a juvenile according to Jensen et al. (2016); *C. caretta* presented CCL of 80 cm and CCW of 76 cm, a sub-adult, according to Dood (1988); *E. imbricata* presented CCL of 88.5 cm and CCW of 79.5 cm, an adult, according to Ferreira et al. (2018); finally, *L. olivacea* presented CCL of 74.5 and CCW of 72.7 cm also an adult, according to Márquez (1990).

Detailed results of Hg concentrations in the scutes of the four species can be found in Table S1. Preliminary inspection of the data indicated that Hg concentrations were not different between left and right sides of costal and marginal scutes for all species, therefore we pooled the data for these areas. In summary, Hg concentrations found in *C. mydas* scutes varied from 317 to 485.6 ng g⁻¹ (n = 30) with an average of 380.4 ± 63.2 ng g⁻¹ (Fig. 2). Hg concentrations were significantly different among carapace areas in *C. mydas* (Kruskal-Wallis, chi-squared = 21.1, df = 2, p < 0.01) but were higher in vertebral scutes (Mann Whitney post hoc test, p < 0.01) followed by marginal and costal areas between which no difference in Hg concentrations was observed (Mann Whitney post hoc test, p > 0.01). Similarly, in *E. imbricata*, Hg concentrations varied from 5.7 to 17.5 ng g⁻¹ (n = 18) with an average of 10.8 ± 3.4 ng g⁻¹ (Fig. 2). Hg concentrations

Fig. 2 Comparative boxplot of Hg concentrations in vertebral (VS), costal (CS), and marginal scutes (MS) of *C. mydas* (A), *C. caretta* (B), *E. imbricata* (C), and *L. olivacea* (D). The boxplot for *C. caretta* shows the outliers because it did not interfere with the statistical analyses



were significantly different among carapace areas of *E. imbricata* (ANOVA: $F_{2,16} = 6.8$, $p < 0.01$) and higher in the vertebral area (Tukey post hoc test, $P < 0.01$) followed by marginal and costal scutes between which no significant differences were observed (Tukey post hoc test, $p = 0.08$). In *C. caretta*, Hg concentrations varied from 86.0 to 407.8 ng g⁻¹ ($n = 30$) with an average of 262.1 ± 87.5 ng g⁻¹ (Fig. 2). No significant differences in Hg concentrations between vertebral and costal carapace areas were found for *C. caretta* (ANOVA: $F_{1,28} = 4.1$, $p > 0.01$) (Fig. 2). Lastly, Concentrations of Hg in *L. olivacea* varied between 311.0 and 559.2 ng g⁻¹ ($n = 18$) with an average of 434.8 ± 82.3 ng g⁻¹. No significant differences in Hg concentrations between vertebral and marginal carapace areas were found for *L. olivacea* (ANOVA: $F_{1,16} = 0.2$, $p = 0.67$). Unfortunately, due to the small number of sampled individuals, a species-to-species comparison of the Hg content is not possible. Still, *E. imbricata* showed remarkable lower Hg concentrations compared to the other three species, which will be briefly discussed in the following section.

Discussion

Scutes reflect internal Hg burdens by the good correlation of Hg levels between scutes and internal organs (Sakai et al. 2000; Bezerra et al. 2013; Schneider et al. 2015; Villa et al. 2019). However, there are still some aspects about the use of

scutes that need to be assessed to establish an adequate sampling methodology. Among these, a possible variation of Hg concentrations across carapace areas (scutes from vertebral, costal, and marginal areas), is of utmost importance. Mattei et al. (2015), for example, show the first mapping of the concentrations of eleven metals (Pb, Ca, U, Zn, Mn, Mg, Sb, Cr, Cu, Cd, and V) in the carapace of a juvenile individual of *C. caretta* sampled in the Mediterranean, and they also observed spatial differences. However, these authors did not report Hg concentrations, and unlike our work where we collected the keratinized layer, the samples were collected using core drill and probably also include different layers such as dermis and bone.

Our results showed that there is indeed a variation in Hg concentrations, with higher concentrations observed in vertebral scutes when compared to other areas of the carapace in at least two of the studied species. The causes for this variation can be associated with the growth and ossification processes of marine turtle's carapace, as was found by Mattei et al. (2015).

The thickness of the scutes varies depending on their location in the carapace, whether in the vertebral, costal, or marginal areas (López-Castro et al. 2014). In *C. mydas* and *C. caretta*, the vertebral area is the thickest and consequently shows a longer historical record of environmental changes detectable through biochemical markers, stable isotopes, and trace metal concentrations (López-Castro et al. 2014). Thus, keratin layers sampled at different depths

and locations may reflect different periods of deposition and accumulation of trace metals such as Hg (Day et al. 2005). Furthermore, the origin of the carapace is a very interesting factor that needs to be assessed. This structure is derived from its endoskeleton, where the vertebral area is ossified first, and then from this, the ribs originate (Hirasawa et al. 2013; Mattei et al. 2015). Thus, the process of carapace formation apparently may have a direct relationship with the magnitude of trace metal concentrations, as suggested by the different distribution of Hg concentrations observed in this present study.

Mapping of metal concentrations in the carapace is essential to understand its distribution and improve sampling methodologies in these reptiles. Differences in metal accumulation across carapace areas can be explained by the progressive ossification of the carapace during growth, where the central part ossifies first, accumulating metals for longer periods and, therefore, showing higher concentration (Mattei et al. 2015). While the coastal areas reflect the low concentrations that result from a relatively more recent exposure compared to the vertebral area (Mattei et al. 2015). According to these authors, the highest concentrations of metals in vertebral scutes strongly correlated with the longer exposure time, relative to scutes in other areas of the carapace, 0.8 years in juveniles and 6.5 years in adults (Vander Zanden et al. 2013).

The distribution of Hg concentrations in the sub-adult individual of *C. caretta* from the present study did not differ across carapace area as observed by Mattei et al. (2015) for other metals. Scutes are continuously produced over the entire surface of the carapace; hence, as the animal grows and the bony shell increases in area, scutes become thicker over the older areas (e.g., vertebral area) while areas of recent growth expansion are covered only by thin, younger scute tissues (e.g., costal, and marginal areas). Scutes tissues are inert and, although are susceptible to wear and shedding, they retain a record of diet and feeding habitat, (Alibardi 2005; Reich et al. 2007). Thus, individuals in different life stages may show a more recent keratin layer which in turn can generate differences in the pattern of metal concentration in the carapace and contribute to the difference between vertebral scutes and those from other areas.

It is widely known that sea turtles are endangered species, which is why it is essential to find non-invasive and reliable methodologies that allow the use of these organisms as monitors of Hg in oceans and coastal areas (Faust et al. 2014; López-Castro et al. 2014; Barraza et al. 2019). Our results showed spatial variation in Hg concentrations related to the form of carapace growth. Depending on the area where the scutes will be collected, a pattern of Hg concentration can be found that will be linked to older or more recent deposition, and therefore exposure, periods. Although

bioaccumulation in sea turtles is slow and may turn eventual concentration differences negligible, the use of standardized sampling methodologies is still recommended (Day et al. 2005). Thus, the area of the carapace that will be sampled has to be chosen depending on the objective of the study and target species to properly use scutes as a tool to monitor environmental changes on Hg concentrations and even the effects of ontogenetic changes and different diets on the Hg content and exposure of the different species of sea turtles.

Finally, it is well known that diet is the main source of Hg incorporation in marine organisms (Gray 2002). We found the Hg levels were in a similar range for all studied species, except in *E. imbricata* which presented very low concentrations. Although our results for this single individual cannot be extrapolated to the species level, similarly low Hg levels have been previously reported in scutes of *E. imbricata* (Escobedo-Mondragón et al. 2021, 2023). *E. imbricata* forage on a low trophic level, mainly on sponges, but also on other reef-encrusting organisms (Bjorndal 1997) which may or may not contain low Hg concentrations (e.g., Orani et al. 2020 for sponges, and Rizzini et al. 2016). Therefore, it is necessary to further investigate the diet of the *E. imbricata* population from the present study to better understand these low Hg levels.

The mapping of Hg carried out in this work allowed us to understand the distribution of Hg in the vertebral, costal, and marginal areas. Future monitoring studies should consider the different growing areas of the carapace and choose the area of collection based on the specific study goals. Future studies should also prioritize the collection of samples, keeping the detailed clean protocols and sample handling, and whenever possible always in the same areas and depth of the carapace, avoiding inner tissues such as dermis and bone. This will facilitate comparisons across studies and considering the form of growth of the carapace. Unfortunately, our results are based on the analysis on only one individual of each species, therefore, this limiting aspect shall be considered whenever monitoring strategies are planned.

In the case of *C. mydas*, the use of vertebral scutes is recommended for long-term studies as they show an older record of accumulated Hg. For *C. caretta* and *L. olivacea*, the results did not show significant differences between the costal and marginal areas of the carapace, as for *C. mydas* and *E. imbricata*. The lack of data for the vertebral area did not allow for a clearer idea of the Hg distribution pattern. It is recommended that future studies to carry out a more complete initiative to determine whether there is the same Hg distribution pattern found in *C. mydas* and *E. imbricata*. In studies involving a large number of individuals, it is highly recommended that the sampling always be carried out in the same area of the carapace. Our results were based on two

adults, one subadult, and one juvenile individual, so it is essential to also map Hg in the carapace of different life stages of the same species to determine whether the Hg distribution pattern can change according to the individual's life stage.

Acknowledgements This research was funded by Fundação Cearense de Apoio ao Desenvolvimento Científico e Tecnológico (FUNCAP) Project No. INT-00159-00009.01.00/19 and the INCT Continent-Ocean Materials Transfer (INCT-TMCOcean CNPq Proc. No. 465.290/2014-0), and Proc. No. 405.244/2018-5 and 309.718/2016-3 to LD Lacerda. We thank team of EcoAssociados (Pernambuco) and Instituto Verdeluz (Ceará) for field work support.

Declarations

Conflict of interest No potential conflict of interest was reported by the authors.

References

- Achrai B, Wagner HD (2013) Micro-structure and mechanical properties of the turtle carapace as a biological composite shield. *Acta Biomater* 9:5890–5902. <https://doi.org/10.1016/j.actbio.2012.12.023>
- Alibardi L (2005) Proliferation in the epidermis of chelonians and growth of the horny scutes. *J Morphol* 265:52–69. <https://doi.org/10.1002/jmor.10337>
- Barraza AD, Komoroske LM, Allen C, Eguchi T, Gossett R, Holland E, Lowe CG (2019) Trace metals in green sea turtles (*Chelonia mydas*) inhabiting two southern California coastal estuaries. *Chemosphere* 223:342–350. <https://doi.org/10.1016/j.chemosphere.2019.01.107>
- Bellini C, Santos AJ, Grossman A, Marcovaldi MA, Barata PC (2013) Green turtle (*Chelonia mydas*) nesting on atol das Rocas, northeastern Brazil, 1990–2008. *J Mar Biol Association United Kingdom* 93(4):1117–1132. <https://doi.org/10.1017/S002531541200046X>
- Bezerra MF, Lacerda LD, Costa BG, Lima EH (2012) Mercury in the sea turtle *Chelonia mydas* (Linnaeus, 1958) from Ceará coast, NE Brazil. *An Acad Bras Ciênc* 84:123–128. <https://doi.org/10.1590/S0001-37652012000100012>
- Bezerra MF, Lacerda LD, Lima EHSM, Melo MTD (2013) Monitoring mercury in green sea turtles using keratinized carapace fragments (scutes). *Mar Pollut Bull* 77:424–427. <https://doi.org/10.1016/j.marpolbul.2013.09.020>
- Bezerra MF, Lacerda LD, Rezende CE, Franco MAL, Almeida MG, Macêdo GR, Lopez GG (2015) Food preferences and hg distribution in *Chelonia mydas* assessed by stable isotopes. *Environ Pollut* 206:236–246. <https://doi.org/10.1016/j.envpol.2015.07.011>
- Bjorndal KA (1997) Foraging ecology and nutrition of sea turtles. The biology of sea turtles. CRC Press, Boca Raton, FL, pp 199–231
- Bruno DA, Willmer IQ, Pereira LHSdS, Rocha RCC, Saint'Pierre TD, Baldassin P, Scarelli ACS, Tadeu AD, Correia FV, Saggiaro EM, Lemos LS, Siciliano S, Hauser-Davis RA (2021) Metal and metalloid contamination in green sea turtles (*Chelonia mydas*) found stranded in Southeastern Brazil. *Front Mar Sci* 8:608253. <https://doi.org/10.3389/fmars.2021.608253>
- Day RD, Christopher SJ, Becker PR, Whitaker DW (2005) Monitoring mercury in the loggerhead sea turtle, *Caretta caretta*. *Environ Sci Technol* 39:437–446. <https://doi.org/10.1021/es049628q>
- Escobedo-Mondragón M, Luzardo OP, Zumbado M, Rodríguez-Hernández Á, Rial Berriel C, Ramírez-Gomez HV, González-Rebeles Islas C, Aguilar Fisher RF, Rosiles Martínez JR (2021) Incidence of 49 elements in the blood and scutes tissues of nesting hawksbill turtles (*Eretmochelys imbricata*) in Holbox Island. 41:101566. *Regional Studies in Marine Science* <https://doi.org/10.1016/j.rsma.2020.101566>
- Escobedo-Mondragón M, Luzardo OP, Henríquez-Hernández LA, Rodríguez-Hernández A, Zumbado M, Martínez JRR, Farias FG, Suzán G, González-Rebeles Islas C (2023) Trophic behavior of inorganic elements in nesting sea turtles (*Chelonia mydas*, *Eretmochelys imbricata*, and *Caretta caretta*) in Quintana Roo: Biomagnification and biodilution effect in blood and scute tissues. *Mar Pollut Bull* 187:114582. <https://doi.org/10.1016/j.marpolbul.2023.114582>
- Evers DC, Taylor M, Burton M, Johnson S (2018) Mercury in the Global Environment: Understanding spatial patterns for biomonitoring needs of the Minamata Convention on Mercury. *Biodiversity Research Institute. BRI Science Communications Series* 2018-21, Portland, Maine, 21 p
- Faust DR, Hooper MJ, Cobb GP, Barnes M, Shaver D, Ertolacci S, Smith PN (2014) Inorganic elements in green sea turtles (*Chelonia mydas*): Relationships among external and internal tissues. *Environ Toxicol Chem* 33(9):2020–2027. <https://doi.org/10.1002/etc.2650>
- Gray JS (2002) Biomagnification in marine systems: the perspective of an ecologist. *Mar Pollut Bull* 45:46–52. [https://doi.org/10.1016/S0025-326X\(01\)00323-X](https://doi.org/10.1016/S0025-326X(01)00323-X)
- Hirasawa T, Nagashima H, Kuratani S (2013) The endoskeletal origin of the turtle carapace. *Nat Commun* 4:1–7. <https://doi.org/10.1038/ncomms3107>
- Jensen MP, Bell I, Limpus CJ, Hamann M, Ambar S, Whap T, Fitz Simmons NN (2016) Spatial and temporal genetic variation among size classes of green turtles (*Chelonia mydas*) provides information on oceanic dispersal and population dynamics. *Mar Ecol Prog Ser* 543:241–256. <https://doi.org/10.3354/meps11521>
- López-Castro MC, Bjorndal KA, Bolten AB (2014) Evaluation of scute thickness to infer life history records in the carapace of green and loggerhead turtles. *Endanger Species Res* 24:191–196. <https://doi.org/10.3354/esr00593>
- Marcovaldi M, Lopez GG, Soares LS, Lima EH, Thomé JC, Almeida AP (2010) Satellite-tracking of female loggerhead turtles highlights fidelity behavior in northeastern Brazil. *Endanger Species Res* 12(3):263–272. <https://doi.org/10.3354/esr00308>
- Marins RV, Paula Filho FJD, Maia SRR, Lacerda LDD, Marques WS (2004) Distribuição de mercúrio total como indicador de poluição urbana e industrial na costa brasileira. *Química Nova* 27:763–770. <https://doi.org/10.1590/S0100-40422004000500016>
- Márquez RM (1990) Sea Turtles of the world: an annotated and illustrated catalog of sea turtle species known to date. FAO, Rome
- Mattei D, Veschetti E, D'Ilio S, Blasi MF (2015) Mapping elements distribution in carapace of *Caretta caretta*: a strategy for biomonitoring contamination in sea turtles? *Mar. Pollut Bull* 98:341–348. <https://doi.org/10.1016/j.marpolbul.2015.06.001>
- Moura CCM, Guimarães ES, Moura GJB, Amaral GJA, Silva AC (2012) Distribuição espaço-temporal e sucesso reprodutivo de *Eretmochelys imbricata* nas praias do Ipojuca. *Pernambuco Brasil Iheringia Série Zoologia* 102(3):254–260. <https://doi.org/10.1590/S0073-47212012005000003>
- Needham LL, Calafat AM, Barr DB (2008) Assessing developmental toxicant exposures via biomonitoring. *Bas Clin Pharmacol Toxicol* 102:100–108. <https://doi.org/10.1111/j.1742-7843.2007.00185.x>
- Orani AM, Vassileva E, Azemard S, Thomas OP (2020) Comparative study on hg bioaccumulation and biotransformation in Mediterranean and Atlantic sponge species. *Chemosphere* 260:127515. <https://doi.org/10.1016/j.chemosphere.2020.127515>

- Proietti MC, Lara-Ruiz P, Reisser JW, Pinto LS, Dellagostin OA, Marins LF (2009) Green turtles (*Chelonia mydas*) foraging at Arvoredo Island in Southern Brazil: genetic characterization and mixed stock analysis through mtDNA control region haplotypes. *Genet Mol Biology* 32(3):613–618. <https://doi.org/10.1590/S1415-47522009000300027>
- Reich KJ, Bjorndal KA, Bolten AB (2007) The ‘lost years’ of green turtles: using stable isotopes to study cryptic life stages. *Biol Lett* 3:712–714. <https://doi.org/10.1098/rsbl.2007.0394>
- Rizzini AN, Fernandez MA, Brito JL, Vidal LG, Costa ESA, Malm O (2016) Assessing mercury contamination in a tropical coastal system using the mussel *Perna perna* and the sea anemone *Bunodosoma caissarum*. *Environ Monit Assess* 188, 679 (2016). <https://doi.org/10.1007/s10661-016-5683-7>
- Rodriguez CAB, Bezerra MF, Rezende CED, Bastos WR, Lacerda LD (2019) Mercury and methylmercury in carapace of the marine turtle *Caretta caretta*, in northeastern Brazil and its potential for monitoring. *An Acad Bras Ciênc* 91:e20180672. <https://doi.org/10.1590/0001-3765201920180672>
- Sakai H, Saeki K, Ichihashi H, Suganuma H, Tanabe S, Tatsukawa R (2000) Species-specific distribution of heavy metals in tissues and organs of loggerhead turtle (*Caretta caretta*) and green turtle (*Chelonia mydas*) from Japanese coastal waters. *Mar Pollut Bull* 40:701–709. [https://doi.org/10.1016/S0025-326X\(00\)00008-4](https://doi.org/10.1016/S0025-326X(00)00008-4)
- Sales G, Giffoni BB, Barata PC (2008) Incidental catch of sea turtles by the Brazilian pelagic longline fishery. *J Mar Biol Association United Kingdom* 88(4):853–864. <https://doi.org/10.1017/S0025315408000441>
- Schneider L, Eggins S, Maher W, Vogt RC, Krikowa F, Kinsley L, Da Silveira R (2015) An evaluation of the use of reptile dermal scutes as a non-invasive method to monitor mercury concentrations in the environment. *Chemosphere* 119:163–170. <https://doi.org/10.1016/j.chemosphere.2014.05.065>
- Toni M, Dalla Valle L, Alibardi L (2007) Hard (beta-) keratins in the epidermis of reptiles: composition, sequence, and molecular organization. *J Proteome Res* 6:3377–3392. <https://doi.org/10.1021/pr0702619>
- Vander Zanden HB, Bjorndal KA, Bolten AB (2013) Temporal consistency and individual specialization in resource use by green turtles in successive life stages. *Oecologia* 173:767–777. <https://doi.org/10.1007/s00442-013-2655-2>
- Vélez-Rubio GM, Cardona L, López-Mendilaharsu M, Martínez Souza G, Carranza A, González-Paredes D, Tomás J (2016) Ontogenetic dietary changes of green turtles (*Chelonia mydas*) in the temperate southwestern Atlantic. *Mar Biol* 163(3):1–16. <https://doi.org/10.1007/s00227-016-2827-9>
- Villa CA, Bell I, Hof CM, Limpus CJ, Gaus C (2019) Elucidating temporal trends in trace element exposure of green turtles (*Chelonia mydas*) using the toxicokinetic differences of blood and scute samples. *Sci Tot Environ* 651:2450–2459. <https://doi.org/10.1016/j.scitotenv.2018.10.092>
- Warner T, Jalilvand F (2016) Formation of hg (II) tetrathionate complexes with cysteine at neutral pH. *Can J Chem* 94:373–379. <https://doi.org/10.1139/cjc-2015-0375>
- Wyneken J (2001) The anatomy of Sea Turtles. U.S. Department of Commerce NOAA Technical Memorandum NMFS-SEFSC. –470:1–172

Publisher's Note Springer Nature remains neutral with regard to jurisdictional claims in published maps and institutional affiliations.

Springer Nature or its licensor (e.g. a society or other partner) holds exclusive rights to this article under a publishing agreement with the author(s) or other rightsholder(s); author self-archiving of the accepted manuscript version of this article is solely governed by the terms of such publishing agreement and applicable law.